COMPUTED TOMOGRAPHY

Photon-counting detector computed tomography for metal artifact reduction: a comparative study of different artifact reduction techniques in patients with orthopedic implants

Fabian Bernhard Pallasch[1] · Alexander Rau[1] · Marco Reisert[1] · Stephan Rau[1] · Thierno Diallo[1] · Thomas Stein[1] · Sebastian Faby[2] · Fabian Bamberg[1] · Jakob Weiss[1]

© The Author(s) 2024

Abstract

Purpose Artifacts caused by metallic implants remain a challenge in computed tomography (CT). We investigated the impact of photon-counting detector computed tomography (PCD-CT) for artifact reduction in patients with orthopedic implants with respect to image quality and diagnostic confidence using different artifact reduction approaches.

Material and methods In this prospective study, consecutive patients with orthopedic implants underwent PCD-CT imaging of the implant area. Four series were reconstructed for each patient (clinical standard reconstruction [PCD-CT$_{Std}$], monoenergetic images at 140 keV [PCD-CT$_{140keV}$], iterative metal artifact reduction (iMAR) corrected [PCD-CT$_{iMAR}$], combination of iMAR and 140 keV monoenergetic [PCD-CT$_{140keV+iMAR}$]). Subsequently, three radiologists evaluated the reconstructions in a random and blinded manner for image quality, artifact severity, anatomy delineation (adjacent and distant), and diagnostic confidence using a 5-point Likert scale (5 = excellent). In addition, the coefficient of variation [CV] and the relative quantitative artifact reduction potential were obtained as objective measures.

Results We enrolled 39 patients with a mean age of 67.3 ± 13.2 years (51%; n = 20 male) and a mean BMI of 26.1 ± 4 kg/m^2. All image quality measures and diagnostic confidence were significantly higher for the iMAR vs. non-iMAR reconstructions (all $p < 0.001$). No significant effect of the different artifact reduction approaches on CV was observed ($p = 0.26$). The quantitative analysis indicated the most effective artifact reduction for the iMAR reconstructions, which was higher than PCD-CT$_{140keV}$ ($p < 0.001$).

Conclusion PCD-CT allows for effective metal artifact reduction in patients with orthopedic implants, resulting in superior image quality and diagnostic confidence with the potential to improve patient management and clinical decision making.

Keywords Multidetector computed tomography · Artifacts · Image processing · Computer-assisted · Arthroplasty, replacement, hip · Spine

Introduction

Artifacts caused by metallic orthopedic implants such as prosthesis and osteosynthesis are an ongoing challenge in computed tomography (CT) imaging, and their prevalence is expected to further increase in an aging population [1, 2]. These artifacts manifest as streaks and shadows around the implant due to photon starvation, photon scattering, and beam hardening [3, 4]. As a result, image quality can be substantially impaired with the risk of obscuring important findings like implant failure, fractures, or malignancies [5, 6]. Consequently, various approaches were developed and studied to overcome these challenges and to effectively reduce artifacts. These approaches include the calculation of virtual monoenergetic reconstructions at high keV, sinogram inpainting, and iterative metal artifact reduction (iMAR) approaches [7–11]. Alone or in combination, these strategies have demonstrated encouraging results in different patient populations (e.g., patients with dental implants, pacemakers,

✉ Fabian Bernhard Pallasch
   Fabian.pallasch@uniklinik-freiburg.de

1 Department of Radiology, University Medical Center Freiburg, Hugstetter Str. 55, 79106 Freiburg im Breisgau, Germany

2 Siemens Healthcare GmbH, Siemensstr. 3, 91301 Forchheim, Germany

cerebral aneurysm clips, and orthopedic implants) and are increasingly used in daily routine to improve clinical decision making [7, 11–15].

With the clinical implementation of photon-counting-detector CT (PCD-CT) in late 2021, a new technology with the potential to fundamentally change CT imaging has become available [16]. Conventional energy-integrating detectors (EID) rely on scintillators to convert photon energy into electric current for image reconstruction. In contrast, photon-counting detectors directly convert the detected signal and allow for counting and measuring individual photons and their respective energy level [17]. As a result, spectral data is intrinsically obtained in each scan with the potential to improve image post-processing compared to the established EID-CT technology [16, 17]. PCD-CT with multiple energy bins present an advantage compared to EID-CT since different energy bins capture distinct attenuation properties. In the context of metal artifact reduction, high energy-bin images exhibit fewer beam artifacts compared to low-energy-bin images and EID-CT [18]. Another advantage is that reflective septa are not required in PCD setup with the potential to reduce radiation dose compared to EID-CT systems [17, 19]. Finally, dual-energy EID-CT systems always require an upfront decision whether to obtain images in dual- or single-energy mode with consequences on available post-processing possibilities. In contrast, PCD-CT data always allows for advanced post-processing in every scan (e.g., high keV reconstructions), which can be useful for further clarification, especially if unexpected findings are detected. This is supported by a constantly growing body of research demonstrating superior image quality for PCD-CT in different clinical applications [20–26].

Therefore, this study aimed to investigate and compare image quality and diagnostic confidence of PCD-CT for metal artifact reduction using different approaches (monoenergetic reconstructions at 140 keV and iMAR algorithm as standalone techniques and combined) in patients with orthopedic implants. We hypothesized that PCD-CT can effectively reduce artifacts allowing for a significantly improved image quality and diagnostic confidence.

Material and methods

Patient population

The local ethics committee approved this retrospective analysis of prospectively acquired data and written informed consent was obtained from all participants. Consecutive oncological patients with orthopedic implants and indication for PCD-CT imaging as part of their routine clinical workup were enrolled in this study between July 11th, 2022 and August 31st, 2022. Patients were excluded if they had contraindications for contrast-enhanced CT imaging such as allergy to iodine contrast agents, renal impairment, and thyroid dysfunction, as well as individuals under 18 years of age.

Imaging protocol and reconstruction parameters

All CT scans were performed in a supine position using a first-generation dual-source PCD-CT system (NAEOTOM Alpha, Siemens Healthcare, Forchheim, Germany). For all patients, portal-venous phase images were acquired 75 s after body weight-adapted contrast agent administration (Ultravist 370 Bayer Healthcare, 1,2 mg/kg; flow 2 ml/s) using a dual-syringe power injector (Medtron, Saarbruecken, Germany) followed by a 20 ml saline bolus (flow 2 ml/s).

CT data were acquired in multi-spectral mode with a pitch of 0.8, a gantry rotation time of 0.25 s, a collimation of 144×0.40 mm, and a CARE keV IQ level = 145 (corresponding to a reference mAS ranging from 55 to 100). In addition, CareDose4D and CARE keV were enabled for all examinations.

For further analyses, four axial series were reconstructed from the acquired multi-spectral data:

(i) Standard reconstruction (PCD-CT$_{Std}$) at a monoenergetic level of 65 keV to simulate a conventional EID-CT image impression of 120 keV with a bone kernel (Br56), a slice thickness and increment of 2 mm, and quantum iterative reconstruction strength 4.

(ii) High keV monoenergetic reconstruction at 140 keV (PCD-CT$_{140keV}$) following previously published results by Anhaus et al. [8], other parameters as in (i).

(iii) IMAR reconstruction (PCD-CT$_{iMAR}$) using a commercially available iMAR algorithm (Siemens Healthineers, Erlangen, Germany), other parameters as in (i). The iMAR algorithm was specifically developed for efficient metal artifact reduction by combining several recently proposed techniques in an iterative process. In detail, beam hardening caused by the implant is addressed through correction and inpainting in raw data space using a normalized sinogram. In addition, a frequency split technique is applied in the image domain for further and robust artifact reduction [10, 27]. There are seven dedicated optimized iMAR algorithms available for hip implants, intracranial coils, thoracic coils, shoulder implants, pacemakers, dental fillings, and extremity implants. For the current study, the hip implant algorithm was used for all patients as no dedicated application for spinal implants is currently available.

(iv) A combined reconstruction applying the iMAR algorithm to monoenergetic reconstructions at 140 keV (PCD-CT$_{140keV+iMAR}$), other parameters as in (i).

Qualitative image analysis

The image quality of all the reconstructions was subjectively evaluated by three radiologists with 2, 3, and 5 years of experience in CT imaging. All ratings were performed on a dedicated workstation equipped with in-house research image processing software (Nora; https://www.nora-imaging.com/). To ensure unbiased reading results, the radiologists independently assessed all reconstructions on 5-point Likert scales, which were presented in a random order and blinded regarding the type of reconstruction.

The following criteria were evaluated (i) overall image quality; (ii) artifact severity; (iii) delineation of adjacent anatomy (vessels, bone, musculature, lymph nodes); and (iv) delineation of distant anatomy (distant muscles, abdominal/pelvic organs, vessels); (v) diagnostic confidence and interpreted as 5 = excellent/no artifacts, 4 = good/minor artifacts, 3 = fair/moderate artifacts, 2 = poor/severe artifacts, 1 = non-diagnostic (see Fig. 1).

Fig. 1 Example of subjective image quality analysis using a 5-Point Likert scale for overall image quality, artifact severity, delineation of adjacent as well as distant anatomy, and diagnostic confidence, which were graded as: Panel 1—non-diagnostic, Panel 2—poor/severe artifacts, Panel 3—fair/moderate artifacts, Panel 4—good/minor artifacts, Panel 5—excellent/no artifacts. Panel 6 displays the ROI measurements for the coefficient of variation (star) and quantitative artifact reduction analysis (circle—placed in the artifact core)

Results are reported for the entire cohort and stratified by hip implants versus spinal osteosyntheses to investigate whether the hip implant iMAR algorithm could be employed as a reliable alternative for the currently lacking dedicated approach for spinal osteosyntheses.

Quantitative analysis

Coefficient of variation (CV)

The CV was calculated to obtain quantitative image measures and examine possible alterations in image signal homogeneity by the different artifact techniques. CV, also known as the relative standard deviation, is a statistical measure used to assess the relative variability of a dataset in relation to its mean. Therefore, a region-of-interest (ROI) 150 mm^2 in size was placed in a distant muscle, which was subjectively least by the artifact. The localization was identical across all reconstructions (PCD-CT_{Std}, PCD-CT_{140keV}, PCD-CT_{iMAR}, PCD-$CT_{140keV+ iMAR}$) and all measurements were performed in a random order and blinded to the type of reconstruction to ensure a reliable comparison. Mean Hounsfield units (HU) and standard deviations (SD) were measured from the ROI and the CV was calculated using the following equation:

$$CV[HU] = SD_{ROI}/ HU_{ROI} \qquad (1)$$

where CV = the coefficient of variation, SD = standard deviation of the ROI, and HU = the mean density in of the ROI.

Quantification of artifact reduction

To quantitatively assess the effectiveness of the different methods for artifact reduction, we calculated the relative change in artifact severity based on changes in HU within the artifact using the PCD-CT_{Std} reconstruction as a reference. Firstly, the image with the most severe artifact was selected (by XX) on the PCD-CT_{Std} reconstruction for all patients. Secondly, the corresponding images in PCD-CT_{140keV}, PCD-CT_{iMAR}, and PCD-$CT_{140keV+iMAR}$ reconstructions were defined. Finally, a circular ROI (150 mm^2) was used to measure the mean HU values within the artifact in all reconstructions (Fig. 1). The relative change in HU values as a ratio between the different artifact reduction techniques was then calculated as follows:

$$Ratio = (PCD - CT_{reduction\_technique}/PCD - CT_{Std})*100 \qquad (2)$$

where ratio = the relative potential for artifact reduction, PCD-$CT_{reduction\_technique}$ = one of the investigated artifact reduction techniques, and PCD-CT_{std} = the standard reconstruction without artifact reduction.

Similar to the qualitative analysis, we conducted a subgroup analysis stratifying hip implants and spinal osteosyntheses.

Statistical analysis

All statistical analyses were performed using the R Foundation for Statistical Computing (version 4.2.1, Vienna, Austria). Continuous variables are given as mean and SD or median and interquartile ranges, as appropriate. Categorical measures are presented as percentages and frequencies. Friedman's ANOVA with post hoc pairwise comparison was calculated to compare the results of the qualitative image analysis for the entire cohort and stratified by patients with hip implants vs. spinal osteosyntheses. For quantitative measures, repeated measure ANOVA followed by post hoc pairwise comparison was conducted. For all comparisons, Bonferroni correction was applied to account for multiple testing. P values were considered to indicate statistical significance if < 0.05.

Results

The final study cohort consisted of 39 consecutive patients with a mean age of 67.2 ± 13.2 years, 51% male, and a mean BMI of 26.1 ± 4 kg/m^2. For all patients, the four types of reconstructions were successfully calculated. No patients were excluded. The mean $CTDI_{vol}$ was 8 ± 4.3 mGy. Detailed patient characteristics are provided in Table 1.

Qualitative analysis

All radiologists completed their reading sessions for all patients and reconstructions. An overview of the results is presented in Table 2.

Friedman's ANOVA revealed a significant effect of the different reconstruction techniques on image quality for all evaluated criteria. Results were as follows: overall image quality (Friedman's Q (df = 3) 23.4; $p < 0.001$), artifact severity (Friedman's Q (df = 3) 26; $p < 0.001$), delineation of adjacent (Friedman's Q (df = 3) 24.6; $p < 0.001$), delineation of distant anatomy (Friedman's Q (df = 3) 18.2; $p < 0.001$); diagnostic confidence (Friedman's Q (df = 3) 21.9; $p < 0.001$). The highest reading scores were found for PCD-$CT_{140keV+iMAR}$ across all evaluated criteria followed by PCD-CT_{iMAR} and the non-iMAR reconstructions. Bonferroni corrected post hoc pairwise testing revealed significantly higher scores for PCD-$CT_{140keV+iMAR}$ vs. PCD-CT_{Std} (all $p \leq 0.006$) and except for diagnostic confidence ($p = 0.06$) PCD-CT_{iMAR} versus PCD-CT_{Std} were significant ($p \leq 0.02$). Scores for PCD-CT_{140keV} were significantly

Table 1 Patient characteristics and radiation dose

Variable	N (%) or mean $\pm$ SD
Participants	39 (100%)
Sex (male)	20 (51%)
Age (years)	67.2 $\pm$ 13.2
Weight (kg)	74.3 $\pm$ 14
Height (meter)	1.69 $\pm$ 0.1
BMI (kg/m^2)	26.1 $\pm$ 4
Metallic implants	
Spinal osteosynthesis	13 (33.3%)
Hip replacement	13 (33.3%)
Osteosynthesis	9 (23%)
Knee replacement	2 (5.1%)
Shoulder replacement	2 (5.1%)
Clinical diagnosis	
GI-cancer	8 (20.5%)
Orthopedic	8 (20.5%)
Breast cancer	6 (15.4%)
Vascular	6 (15.4%)
Lung cancer	6 (15.4%)
Hematologic neoplasia	5 (12.8%)
Radiation dose	
CTDIvol (mGy)	8 $\pm$ 4.3

higher compared to PCD-CT$_{Std}$ for the assessment of the distant anatomy ($p = 0.02$). A representative example is given in Table 2.

Subgroup analysis stratified by hip replacements vs. spinal osteosyntheses revealed a similar pattern for patients with hip replacements (Table S1, image example for hip replacement Fig. 2). For spinal osteosynthesis, reading scores for PCD-CT$_{140keV}$ were substantially higher compared to the hip replacement analysis resulting in significant differences vs. PCD-CT$_{Std}$ similar to PCD-CT$_{iMAR}$ and PCD-CT$_{iMAR+140\,keV}$, which was not seen for patients with hip replacements (Table S2, image example for spinal osteosynthesis Fig. 3).

Quantitative image analysis

Coefficient of variation

Mean CV values were 0.79 ± 1.2 for PCD-CT$_{Std}$, 0.45 ± 0.55 for PCD-CT$_{140keV}$, 0.56 ± 0.93 for PCD-CT$_{iMAR} = 0.61 \pm 0.67$, and PCD-CT$_{140keV+iMAR}$. No significant effect for the type of reconstruction on signal homogeneity was noted (repeated measure ANOVA: F value $= 1.34$; df $= 3$; $p = 0.26$). An overview is provided in Fig. 4.

Quantification of artifact reduction

Repeated measure ANOVA indicated a significant impact for the type of reconstruction on artifact severity (F value $= 270$; df $= 3$; $p < 0.001$). Relative changes in HU values were as follows: PCD-CT$_{140keV} = 38 \pm 28.7$, PCD-CT$_{iMAR} = 13.5 \pm 10.8$ and PCD-CT$_{140keV+iMAR} = 9.6 \pm 7.9$ with PCD-CT$_{Std} = 100 \pm 0.0$ serving as reference. Post hoc pairwise testing showed a significant difference in artifact reduction potential between the iMAR and non-iMAR reconstructions (all $p < 0.001$), whereas no significant difference was found between PCD-CT$_{iMAR}$ vs. PCD-CT$_{iMAR+140\,keV}$ ($p = 0.69$). A summary is presented in Fig. 5a.

Similar results were found in subgroup analysis stratified by hip replacements and spinal osteosyntheses with the only difference that PCD-CT$_{140keV}$ facilitated a more severe artifact reduction in patients with spinal osteosyntheses compared to hip replacements (Fig. 5b and c).

Discussion

This study explored the value of several metal artifact reduction approaches in patients with orthopedic implants using a clinically approved PCD-CT system. Our results indicate that artifacts could be significantly reduced with a dedicated iMAR algorithm as a standalone technique. Combining the iMAR approach with high keV monogenetic reconstructions at 140 keV resulted in a further improvement of image quality and diagnostic confidence compared to the clinical standard reconstruction, whereas monoenergetic images at 140 keV alone only provided satisfying results in patients with spinal osteosyntheses but not in patients with hip replacements.

This is of clinical relevance to account for impaired image quality caused by metallic implants. For orthopedic hardware, assessment of the implant itself as well as of the surrounding anatomy is clinically important to ensure the integrity of the implant and to detect potentially relevant findings in proximity that might otherwise go unnoticed [28]. In line with previous studies using conventional EID-CT systems, our results indicate that the tested iMAR algorithm alone and in combination with monoenergetic imaging at 140 keV is an effective approach to address this clinical need by providing improved image quality and diagnostic confidence compared to the standard reconstruction. This was found to be true for all evaluated subjective image criteria for iMAR as a standalone technique and could be further improved in combination with high keV monoenergetic reconstructions at 140 keV. PCT-CT$_{140keV}$ alone did not yield significantly higher reading scores compared to the PCD-CT$_{Std}$ in the entire cohort and

Table 2 Results of the qualitative image analysis

	PCD-CT$_{std}$	PCD-CT$_{140\,keV}$	PCD-CT$_{iMAR}$	PCD-CT$_{140keV+iMAR}$
Image quality	3 [2.7–3]	3.7 [3.2–3.7]	4 [3.5–4.3]	4.3 [3.8–4.67]
Comparison				
PCD-CT$_{std}$	–			
PCD-CT$_{140\,keV}$	$p = 0.25$	–		
PCD-CT$_{iMAR}$	$p = 0.003$	$p = 0.25$	–	
PCD-CT$_{140keV+iMAR}$	$p < 0.001$	$p = 0.051$	$p = 1$	–
Artifact severity	2 [1.7–2.3]	3 [2.5–3.7]	3.7 [3–4]	4 [3.3–4.7]
Comparison				
PCD-CT$_{std}$	–			
PCD-CT$_{140\,keV}$	$p = 0.25$	–		
PCD-CT$_{iMAR}$	$p < 0.01$	$p = 0.52$	–	
PCD-CT$_{140keV+iMAR}$	$p < 0.01$	$p = 0.25$	$p = 1$	–
Adjacent anatomy	2 [1.7–2.3]	3 [2.5–3.7]	3.7 [3–4]	4 [3.3–4.7]
Comparison				
PCD-CT$_{std}$	–			
PCD-CT$_{140\,keV}$	$p = 0.92$	–		
PCD-CT$_{iMAR}$	$p < 0.01$	$p = 0.27$	–	
PCD-CT$_{140keV+iMAR}$	$p < 0.001$	$p < 0.01$	$p = 0.43$	–
Distant anatomy	2 [1.7–2.3]	3 [2.5–3.7]	3.7 [3–4]	4 [3.3–4.7]
Comparison				
PCD-CT$_{std}$	–			
PCD-CT$_{140\,keV}$	$p = 0.02$	–		
PCD-CT$_{iMAR}$	$p = 0.02$	$p = 1$	–	
PCD-CT$_{140keV+iMAR}$	$p < 0.001$	$p = 1$	$p = 0.88$	–
Diagnostic confidence	2 [1.7–2.3]	3 [2.5–3.7]	3.7 [3–4]	4 [3.3–4.7]
Comparison				
PCD-CT$_{std}$	–			
PCD-CT$_{140\,keV}$	$p = 1$	–		
PCD-CT$_{iMAR}$	$p = 0.07$	$p = 0.566$	–	
PCD-CT$_{140keV+iMAR}$	$p < 0.001$	$p = 0.003$	$p = 0.28$	–

PCD-CT$_{Std}$ = Standard reconstruction; PCD-CT$_{140keV}$ = virtual monoenergetic reconstruction at 140 keV; PCD-CT$_{iMAR}$ = dedicated iterative metal artifact reduction algorithm; PCD-CT$_{140keV+iMAR}$ = dedicated iterative metal artifact reduction algorithm combined with virtual monoenergetic reconstruction at 140 keV

can therefore not be recommended as an artifact reduction approach if iMAR is available.

However, our subgroup analysis stratified by hip replacement and spinal osteosynthesis revealed that unlike in patients with hip replacements, the 140 keV monoenergetic reconstruction facilitates a significant reduction in artifacts and improvement in image quality compared to the standard reconstruction in patients with spinal osteosynthesis. We attribute this observation to the currently missing iMAR solution optimized for spinal osteosynthesis, which makes high keV monoenergetic reconstructions a valuable alternative in those patients. These results are corroborated by a recent study on the potential of 130 keV monoenergetic reconstructions for metal artifact reduction in 32 patients with spinal osteosynthesis that also described significantly improved image quality and reduced artifacts [29].

The results of the current study complement previous investigations on metal artifact reduction using EID-CT systems. For example, Bongers et al. reported in a study including 46 patients with hip or dental implants using a second-generation dual-source CT scanner that iMAR and virtual monoenergetic reconstructions at 130 keV significantly improved subjective image quality with iMAR yielding superior results compared to the 130 keV reconstructions [15]. Another study by Han et al. including 33
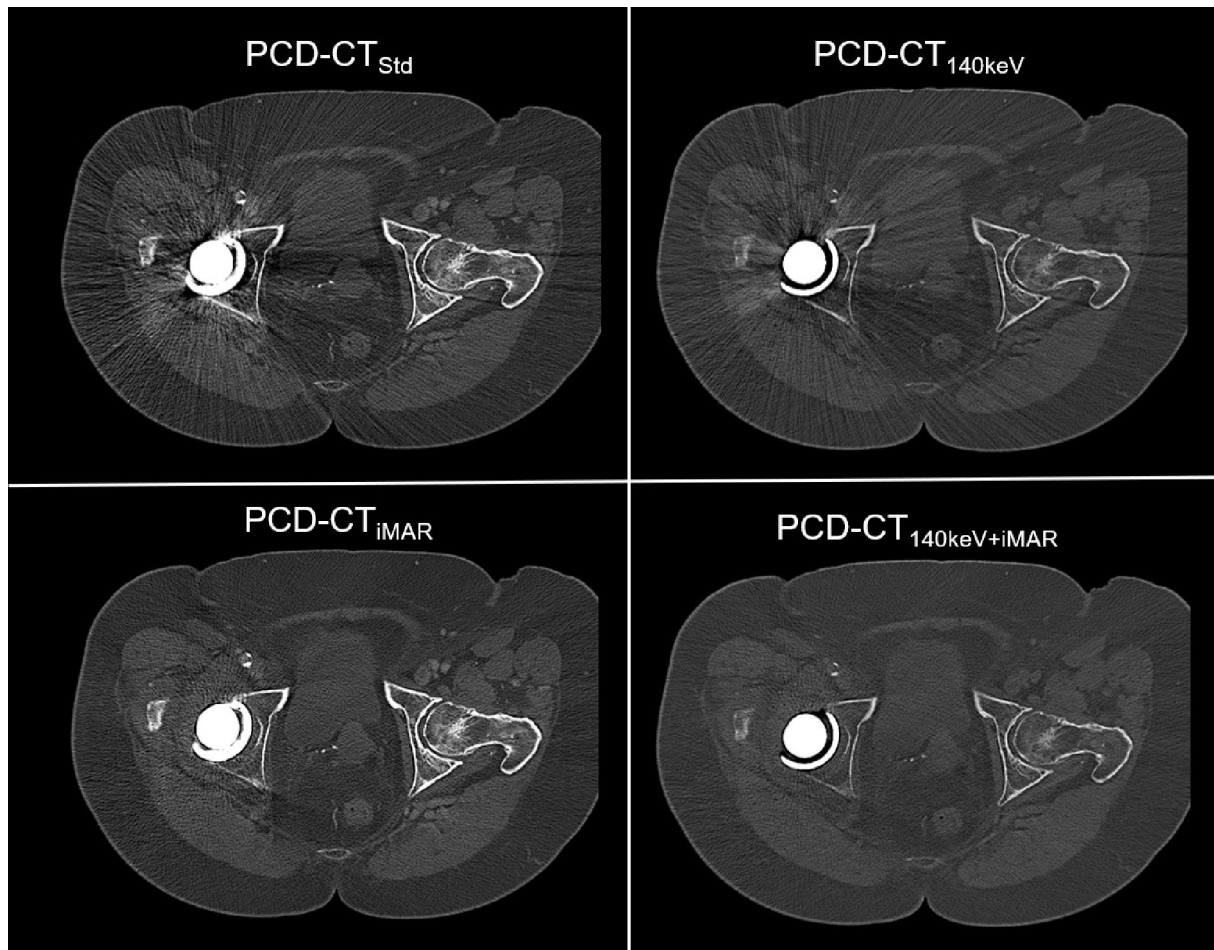
Fig. 2 Image example of a 71-year-old patient with non-small cell lung cancer and hip replacement on the right side. While PCD-CT_{140keV} only provided minor artifact reduction PCD-CT_{iMAR} and PCD-$CT_{iMAR+140\ keV}$ showed substantially more effective artifact reduction. PCD-CT_{Std} = Standard reconstruction; PCD- CT_{140keV} = virtual monoenergetic reconstruction at 140 keV; PCD-CT_{iMAR} = dedicated iterative metal artifact reduction algorithm; PCD-$CT_{140keV+iMAR}$ = dedicated iterative metal artifact reduction algorithm combined with virtual monoenergetic reconstruction at 140 keV

patients with hip implants and 20 patients as controls found increased diagnostic confidence for the pelvic cavity in abdominopelvic CT scans with a dedicated metal artifact reduction software [30]. Similar results were found in initial studies using PCD-CT data, in which high keV monoenergetic reconstruction alone and in combination with iMAR allowed for significant artifact reduction and improved image quality in patients with hip replacement [25, 26]. In addition, several recently published studies have reported comparable findings regarding artifact reduction in patients with dental hardware [31–33]. Our results not only support these findings but also provide novel insights into artifact reduction in patients with various osteosynthesis. Firstly,

we provide a systematic qualitative and quantitative analysis of different artifact reduction techniques for orthopedic implants. Secondly, our subanalysis (hip prosthesis vs. spinal implants) reveals that depending on which anatomical region is examined, the performance of the different artifact reduction techniques provide significantly different results, which has not yet been investigated for PCD-CT and needs to be considered during image reconstruction.

Reliable and effective artifact reduction techniques are also of interest for the expected adoption of novel data analysis strategies. Clinical implementation of artificial intelligence and quantitative image analysis tools is of increasing importance to support clinical workflows in handling the

Fig. 3 Image example of a 76-year-old patient with breast cancer and spinal osteosynthesis. PCD-CT$_{140keV}$ demonstrated superior artifact reduction for spinal osteosynthesis compared to iMAR alone; most effective artifact reduction was achieved with PCD-CT$_{140keV + iMAR}$ likely because there is currently no dedicated spinal iMAR algorithm available. PCD-CT$_{Std}$ = Standard reconstruction; PCD-CT$_{140keV}$ = virtual monoenergetic reconstruction at 140 keV; PCD-CT$_{iMAR}$ = dedicated iterative metal artifact reduction algorithm; PCD-CT$_{140keV+iMAR}$ = dedicated iterative metal artifact reduction algorithm combined with virtual monoenergetic reconstruction at 140 keV
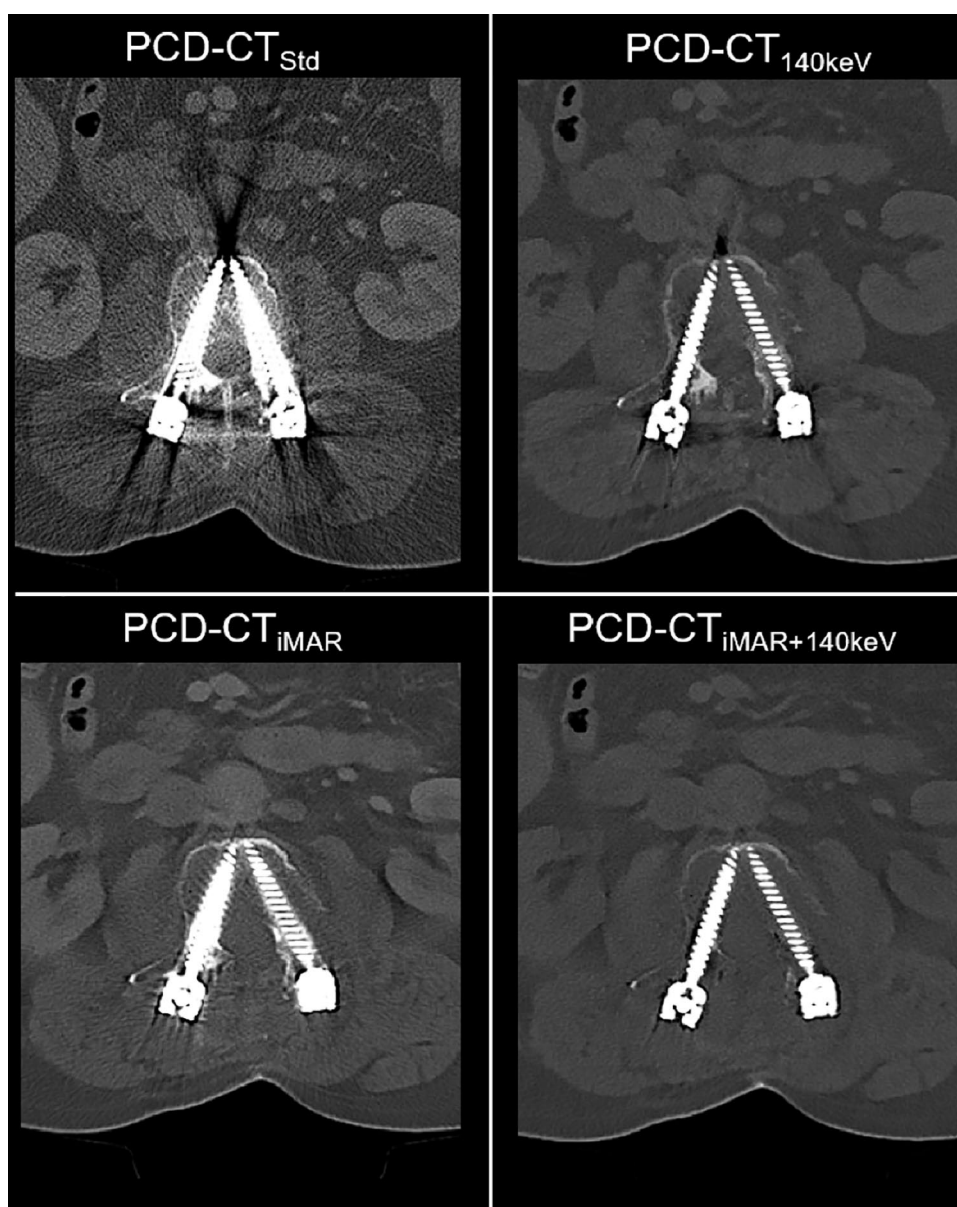
constantly growing amount of data acquired in daily care [34]. However, to ensure accurate and reliable post-processing results, robust input data for the analysis tools is required to avoid potentially erroneous output. Image manipulation, such as artifact reduction, poses the risk of altering the image signal/homogeneity of input data. In our CV analysis, we demonstrated that neither the iMAR approach nor the monoenergetic reconstructions significantly change the original image signal, which could be a relevant limitation for downstream post-processing tasks.

The study has the following limitations. We investigated a spectrum of different orthopedic hardware without further knowledge about vendor and material composition. Further, we included consecutive patients to investigate the artifact reduction potential of the different investigated approaches. As no implant-related findings were found in our relatively small study cohort, more focused studies are needed to assess and compare how often the artifact reduction techniques provide added value and change patient management. Further, not systematic assessment of

Fig. 4 Results of the coefficient of variation analysis as a measure to estimate signal homogeneity. ANOVA revealed no significant impact of the artifact reduction technique on CV ($p = 0.26$). PCD-CT$_{Std}$ = Standard reconstruction (gray); PCD-CT$_{140keV}$ = virtual monoenergetic reconstruction at 140 keV (blue); PCD-CT$_{iMAR}$ = dedicated iterative metal artifact reduction algorithm (yellow); PCD-CT$_{140keV+iMAR}$ = dedicated iterative metal artifact reduction algorithm combined with virtual monoenergetic reconstruction at 140 keV (green)
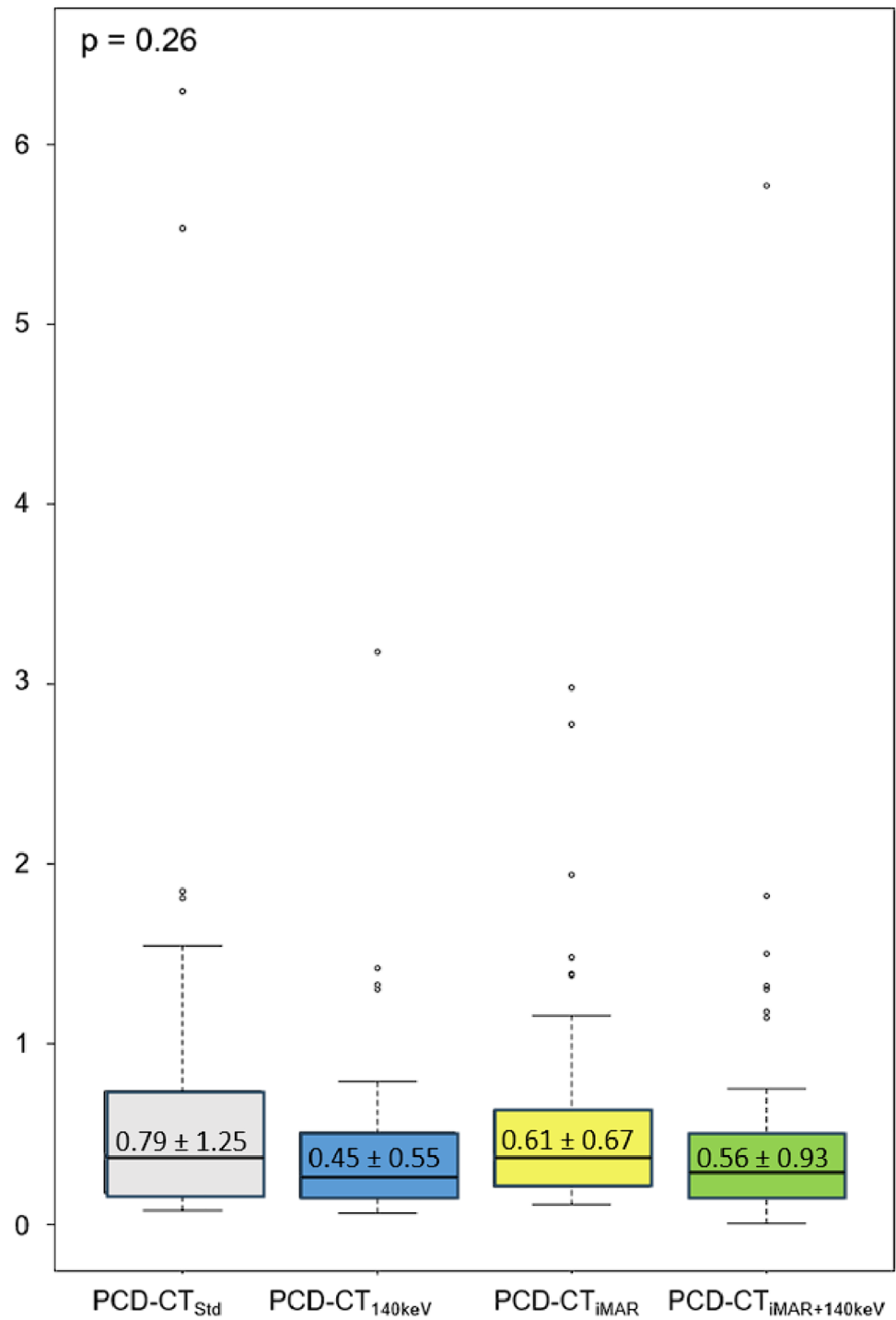
different keV levels was performed. Finally, results of the ratio approach to quantitatively assess the artifact reduction potential need to be interpreted with caution if the HU values of the evaluated region/tissue in the corrected image approaches 0 as this may provide biased results.

In conclusion, PCD-CT allows for effective metal artifact reduction in patients with orthopedic implants resulting in superior image quality and diagnostic confidence with the potential to improve patient management and clinical decision making.

' p >0.05; * p < 0.5; ** p < 0.01; *** p < 0.001; ANOVA p all < 0.001
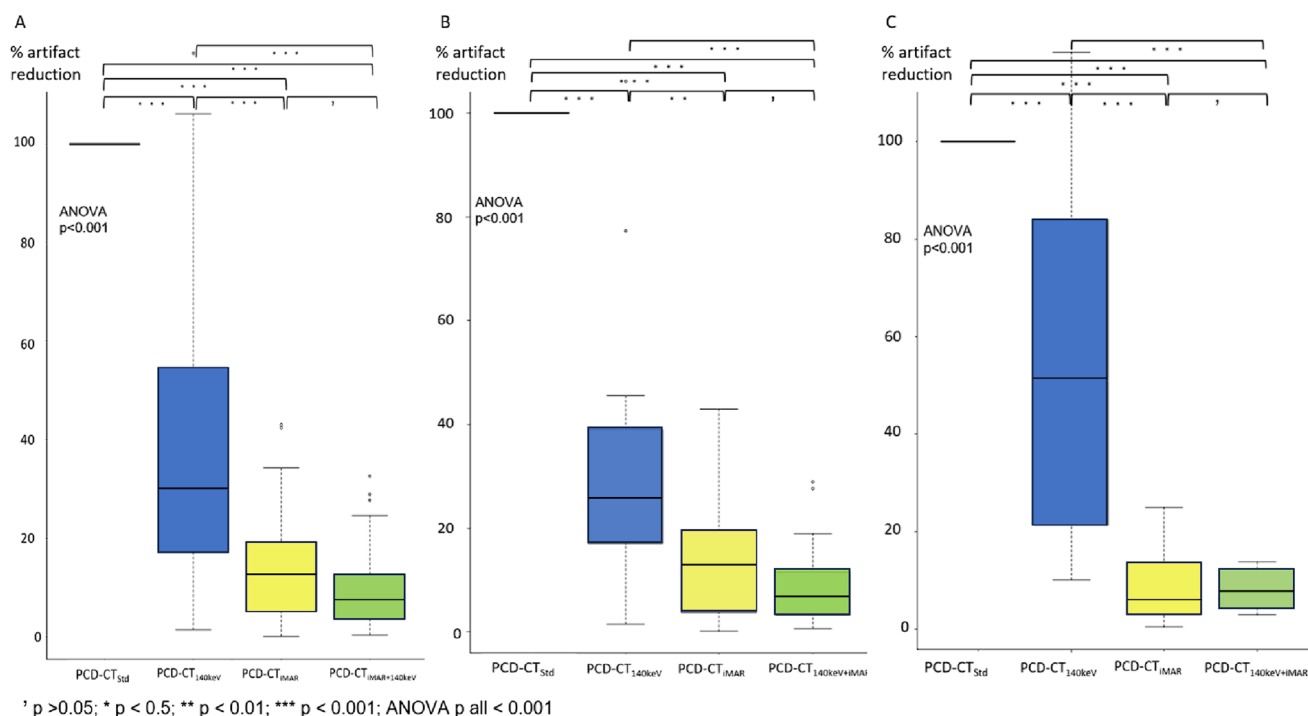
Fig. 5 Results of the HU-based approaches to estimate the quantitative artifact reduction potential of the different investigated techniques. Most effective artifact reduction was achieved by PCT-$CT_{iMAR+140\ keV}$ followed by PCD-CT_{iMAR} and PCD-CT_{140keV}. All p values are corrected for multiple comparisons using Bonferroni correction. **A** entire cohort and stratified by **B** hip replacement and **C** spinal osteosynthesis. PCD-CT_{Std} = Standard reconstruction; PCD-CT_{140keV} = virtual monoenergetic reconstruction at 140 keV; PCD-CT_{iMAR} = dedicated iterative metal artifact reduction algorithm; PCD-$CT_{140keV+iMAR}$ = dedicated iterative metal artifact reduction algorithm combined with virtual monoenergetic reconstruction at 140 keV

Declarations

Conflict of interest Sebastian Faby is employed by Siemens Healthcare GmbH.

Ethical approval This prospective study was approved by the local ethics committee and informed written consent was obtained from all participants.

References

1. Taljanovic MS, Jones MD, Hunter TB et al (2003) Joint arthroplasties and prostheses. Radiographics 23:1295–1314
2. Lee MJ, Kim S, Lee SA et al (2007) Overcoming artifacts from metallic orthopedic implants at high-field-strength MR imaging and multi-detector CT. Radiographics 27:791–803
3. Mori I, Machida Y, Osanai M, Iinuma K (2013) Photon starvation artifacts of X-ray CT: their true cause and a solution. Radiol Phys Technol 6:130–141
4. Boas F, Fleischmann D (2012) CT artifacts: causes and reduction techniques. Imaging Med 4(2):229–240
5. Barrett JF, Keat N (2004) Artifacts in CT: recognition and avoidance. Radiographics 24:1679–1691
6. Baliyan V, Kordbacheh H, Davarpanah AH, Mozafarry A, Sahani DV, Kambadakone A (2019) Orthopedic metallic hardware in routine abdomino-pelvic CT scans: occurrence and clinical significance. Abdominal Radiology 44:1567–1574
7. Abdoli M, Ay MR, Ahmadian A, Dierckx RA, Zaidi H (2010) Reduction of dental filling metallic artifacts in CT-based attenuation correction of PET data using weighted virtual sinograms optimized by a genetic algorithm. Med Phys 37:6166–6177
8. Anhaus JA, Schmidt S, Killermann P, Mahnken A, Hofmann C (2022) Iterative metal artifact reduction on a clinical photon counting system—technical possibilities and reconstruction selection for optimal results dependent on the metal scenario. Phys Med Biol 67:115018
9. Kotsenas AL, Michalak GJ, DeLone DR et al (2015) CT metal artifact reduction in the spine: can an iterative reconstruction

technique improve visualization? AJNR Am J Neuroradiol 36:2184–2190

10. Meyer E, Raupach R, Lell M, Schmidt B, Kachelrieß M (2012) Frequency split metal artifact reduction (FSMAR) in computed tomography. Med Phys 39:1904–1916

11. Weiß J, Schabel C, Bongers M et al (2017) Impact of iterative metal artifact reduction on diagnostic image quality in patients with dental hardware. Acta Radiol 58:279–285

12. Gong XY, Meyer E, Yu XJ et al (2013) Clinical evaluation of the normalized metal artefact reduction algorithm caused by dental fillings in CT. Dentomaxillofac Radiol 42:20120105

13. Park J, Kim SH, Han JK (2019) Combined application of virtual monoenergetic high keV images and the orthopedic metal artifact reduction algorithm (O-MAR): effect on image quality. Abdom Radiol (NY) 44:756–765

14. Bamberg F, Dierks A, Nikolaou K, Reiser MF, Becker CR, Johnson TR (2011) Metal artifact reduction by dual energy computed tomography using monoenergetic extrapolation. Eur Radiol 21:1424–1429

15. Bongers MN, Schabel C, Thomas C et al (2015) Comparison and combination of dual-energy- and iterative-based metal artefact reduction on hip prosthesis and dental implants. PLoS ONE 10:e0143584

16. Esquivel A, Ferrero A, Mileto A et al (2022) Photon-counting detector CT: key points radiologists should know. Korean J Radiol 23:854–865

17. Willemink MJ, Persson M, Pourmorteza A, Pelc NJ, Fleischmann D (2018) Photon-counting CT: technical principles and clinical prospects. Radiology 289:293–312

18. Gutjahr R, Halaweish AF, Yu Z et al (2016) Human imaging with photon counting-based computed tomography at clinical dose levels: contrast-to-noise ratio and cadaver studies. Invest Radiol 51:421–429

19. Yu Z, Leng S, Kappler S et al (2016) Noise performance of low-dose CT: comparison between an energy integrating detector and a photon counting detector using a whole-body research photon counting CT scanner. J Med Imaging 3:043503

20. Bartlett DJ, Koo CW, Bartholmai BJ et al (2019) High-resolution chest computed tomography imaging of the lungs: impact of 1024 matrix reconstruction and photon-counting detector computed tomography. Invest Radiol 54:129–137

21. Symons R, Pourmorteza A, Sandfort V et al (2017) Feasibility of dose-reduced chest CT with photon-counting detectors: initial results in humans. Radiology 285:980–989

22. Symons R, Reich DS, Bagheri M et al (2018) Photon-counting computed tomography for vascular imaging of the head and neck: first in vivo human results. Invest Radiol 53:135–142

23. Soschynski M, Hagen F, Baumann S et al (2022) High temporal resolution dual-source photon-counting CT for coronary artery disease: initial multicenter clinical experience. J Clin Med 11(20):6003

24. Boussel L, Coulon P, Thran A et al (2014) Photon counting spectral CT component analysis of coronary artery atherosclerotic plaque samples. Br J Radiol 87:20130798

25. Layer YC, Mesropyan N, Kupczyk PA et al (2023) Combining iterative metal artifact reduction and virtual monoenergetic images severely reduces hip prosthesis-associated artifacts in photon-counting detector CT. Sci Rep 13:8955

26. Schreck J, Laukamp KR, Niehoff JH et al (2023) Metal artifact reduction in patients with total hip replacements: evaluation of clinical photon counting CT using virtual monoenergetic images. Eur Radiol. https://doi.org/10.1007/s00330-023-09879-4

27. Meyer E, Raupach R, Lell M, Schmidt B, Kachelriess M (2010) Normalized metal artifact reduction (NMAR) in computed tomography. Med Phys 37:5482–5493

28. Trabzonlu TA, Terrazas M, Mozaffary A, Velichko YS, Yaghmai V (2020) Application of iterative metal artifact reduction algorithm to CT urography for patients with hip prostheses. AJR Am J Roentgenol 214:137–143

29. Rau A, Straehle J, Stein T et al (2023) Photon-Counting Computed Tomography (PC-CT) of the spine: impact on diagnostic confidence and radiation dose. Eur Radiol. https://doi.org/10.1007/s00330-023-09511-5

30. Han SC, Chung YE, Lee YH, Park KK, Kim MJ, Kim KW (2014) Metal artifact reduction software used with abdominopelvic dual-energy CT of patients with metal hip prostheses: assessment of image quality and clinical feasibility. AJR Am J Roentgenol 203:788–795

31. Risch F, Decker JA, Popp D et al (2023) Artifact reduction from dental material in photon-counting detector computed tomography data sets based on high-kev monoenergetic imaging and iterative metal artifact reduction reconstructions-can we combine the best of two worlds? Invest Radiol 58:691–696

32. Patzer TS, Kunz AS, Huflage H et al (2023) Combining virtual monoenergetic imaging and iterative metal artifact reduction in first-generation photon-counting computed tomography of patients with dental implants. Eur Radiol 33:7818–7829

33. Pallasch FB, Rau A, Reisert M et al (2023) Impact of different metal artifact reduction techniques in photon-counting computed tomography head and neck scans in patients with dental hardware. Eur Radiol. https://doi.org/10.1007/s00330-023-10430-8

34. Alkadhi H, Euler A (2020) The future of computed tomography: personalized, functional, and precise. Invest Radiol 55:545–555